Synthesis and Characterization of Polyaniline-Polystyrene-Chitosan/Zinc Oxide Hybrid Nanocomposite

Valiollahi, Mir-Hasan; Abbasian, Mojtaba*[+]

Department of Chemistry, Payame Noor University, P. O. Box: 19395-3697 Tehran, .R. IRAN

Pakzad, Mousa

Departments of Chemistry, University of Zanjan, P. O. Box 45195-313, Zanjan, .R. IRAN

ABSTRACT: *A hybrid nanocomposite composed of polyaniline-polystyrene-chitosan/zinc oxide was prepared via a simple in situ polymerization method. The synthesized copolymers were analyzed using Fourier Transform InfraRed (FT-IR), and UltraViolet-Visible (UV–Vis) spectroscopies, ThermoGravimetric Analysis (TGA), and Field Emission Scanning Electron Microscopy (FE-SEM), X-ray diffraction, energy dispersive, X-ray photoelectron spectroscopy and cyclic voltammetry. The chemical bonding established between polyaniline-polystyrene and polyaniline-polystyrene-chitosan/zinc oxide, confirmed by FT-IR, is likely to be responsible for the enhanced chemical stability. From SEM observation, the ratio of ZnO nanoparticles to nanocomposite altered the morphology of the hybrids from granular to plate-like structure, which was confirmed by EDXS. The thermal property was studied using TG/DTA analysis shows the residual weight (TGA curves) and its weight derivative (DTA curves) of the polyaniline-polystyrene-chitosan/zinc oxide are more stable than chitosan and polyaniline-polystyrene-chitosan. Also, the cyclic voltammetry on the obtained hybrid materials revealed that the plate-like structure was more advantages for electrochemical stability. Overall, the results show that the introduction of the ZnO nanoparticles into the polyaniline-polystyrene-chitosan matrix enhanced the thermal and electrode stability.*

KEYWORDS: *Hybride nanocomposite; Polyaniline; Polystyrene; Chitosan; Zinc oxide.*

INTRODUCTION

Over recent years, hybrid materials based on biodegradable polymer have been developed, including conducting polymers, metal nanoparticles, and synthetic polymers, due to excellent properties of individual components and outstanding synergistic effects simultaneously [1-5].

Chitosan (CS) is an abundant natural biopolymer with excellent film-forming abilities, biocompatibility, nontoxicity, good water permeability, high mechanical strength and susceptible to chemical modification due to the presence of reactive hydroxyl and amino functional groups. It is used in a wide range of applications such as wastewater treatments, separation membranes, drug

***** *To whom correspondence should be addressed.*
+ E-mail: m_abbasian20@yahoo.com
1021-9986/2019/5/55-64 *9/$/5.09*

delivery systems, and biosensors. Over recent years, hybrid materials based on CS have been developed, including conducting polymers, metal nanoparticles, and oxide agents, due to the excellent properties of individual components and outstanding synergistic effects simultaneously.

On the other hand, Polyaniline (PANI), polypyrrole, polythiophene, and polyacetylene are some of the important conducting polymers exploited extensively for a variety of applications. Among these, PANI is the most preferred since it can switch between the insulating and conducting phases through an acid/base doping or the de-doping process. PANI has excellent thermal, environmental and electrochemical stability [6]. However, some potential applications have not yet to be exploited because of its poor processability. It is a facile approach to improve its processability by the preparation of composites of the conducting polymers in the processable polymer matrices [7]. These composites, combining the conductivity of the conducting polymers and the processability of the polymer matrices, have been prepared for the various applications, such as sensors [8], electro-conductive hydrogels for biomedical applications [9], anticorrosion coatings, high energy density capacitors, electromechanical devices, EMI shielding materials, catalyst support, and electrode for inhibitive detection of heavy metal ion [10-15].

It was reported that PANI-coated conductive cotton fabrics have potent antibacterial and antifungal activities [16]. In particular, the antibacterial activity of conducting polymer PANI is associated with the ability to act as an electron acceptor or donor. It is explained through the electrostatic adherence between polymer molecules and bacteria, which carry charges of different signs; thus the walls of the bacteria break down and the intracellular fluid leaks out, causing death [17]. However, the use of individual CS and PANI is limited because of its insolubility in water and most organic solvents, thereby making it difficult to process. Additionally, it showed relatively low antifungal activity compared with a commercial fungicide. Hence, numerous researchers tried to improve both solubility and antimicrobial activity of CS and PANI via chemical modification [18]. For example, Chen et al. reported that CS incorporated PANI gives biocompatible chitosan–polyaniline(CS–PANI)matrix, which increases the flexibility and solubility in common solvents for biomedical applications [19] More recently, the introduction of asparagines into CS significantly improved the bactericidal activity and minimum inhibitory concentration, which could be attributed to the higher number of amino groups present in the polymer chain [20]. Compared to organic materials, inorganic materials such as metal oxide nanoparticles possess superior durability, greater selectivity and heat resistance, can produce increased levels of Reactive Oxygen Species (ROS), mostly hydroxyl radicals, H_2O_2 and singlet oxygen, which results in enhanced cell damage. Among the various types of nanomaterials that have been developed, highly ionic nanoparticle- late ZnO nanoparticles are unique with unusual crystal structures, antibacterial and antifungal agents at lower concentrations [21]. Besides, zinc is a mineral element essential to human health and used in the form of ZnO in the daily supplement for zinc. Recently several studies have reported that CS functionalized ZnO nanoparticles are effective at Inhibiting the growth of *Staphylococcusaureus* and *Escherichia* coli [22].

Recently, the interaction of PANI with metal ions has been investigated. One of the most important results was the observed increase in PANI conductivity through interaction with metal ions. This was achieved by reactions of PANI with Lewis acids in anhydrous media [23], with alkali metal salt [24], or with transition metal salt [25]. However, in the case of transition metal ions which could act as oxidizing agents, it was proposed a two-step redox doping mechanism [26]: first, the metal ions oxidize the polymer amine nitrogen atoms; then, the reduced metal ions coordinate to imine nitrogen in the chain backbone; and finally, the reduced cations are oxidized by the imine groups, resulting in the formation of radical cation segments and the corresponding oxidized metal ions.

There were several attempts by our research group and others to improve the performance of chitosan, cellulose, and PANI which depends on structural modification and surface chemistry [27-33]. It was also reported that the addition of iron oxide nanoparticles to the chitosan/PANI films can generate the creatinine biosensor. Among the metal oxide nanoparticles, ZnO has been explored as a potential nanomaterial for biosensing due to their unusual but favorable properties such as high surface area, high catalytic efficiency, non- toxicity, chemical

stability and strong adsorption ability (high isoelectric point pH 9.5 with a wide direct bandgap (3.37 eV) and become excellent electronic and photonic material [34]. In recent years, researchers are more interested in the synthesis of chitosan/ZnO, chitosan/PANI and PANI/ZnO composites [35, 36]. However, there is no more report about the synthesis of chitosan-ZnO-PANI-polystyrene hybrid composites.

In the present work, PANI was prepared via the chemical oxidative polymerization of aniline in the presence of ammonium peroxydisulfate with Maleic Acid (MA) as a dopant. Then for improvement in PANI processability, the PANI-/polystyrene (PANI-PS) composite was prepared *via* in situ radical bulk polymerization of styrene (St) in the presence of benzoyl peroxide (BPO) and the maleic acid doped PANI. In the following, the nanocomposite of chitosan / Zinc oxid was synthesized and finally hybrid nanocomposite of polyaniline-polystyrene-chitosan/zinc oxide was obtained through the incorporation of chitosan / Zinc oxide nanocomposite to PANI-PS composite.

EXPERIMENTAL SECTION

Materials

St (Merck Co.) was dried over anhydrous sodium sulfate and distilled under reduced pressure before use. Aniline (Aldrich chemicals) was distilled twice under reduced pressure before use. Ammonium peroxydisulfate, maleic anhydride, and chitosan (Aldrich chemicals) were used as received. BPO was obtained from Merck Co., recrystallization from chloroform and dried at room temperature in a vacuum oven and finally, stored in a freezer. All other reagents were purchased from Merck Co.

Instrumentation

Ultraviolet-visible absorption spectrum (UV-vis) was obtained by SHIMADZU,UV-2401pc (Shimadzu, Kyoto, Japan). ThermoGravimetric Analysis (TGA) of the nanocomposite was obtained with Linseys TGA PT1000 (linseys, Germany) instrument. About 10 mg of the sample was heated between 25 and 800°C at a rate of 10 °C min^{-1} under flowing nitrogen. The entire test was performed under nitrogen purging at a flow rate of 50 mL/min. X-Ray Diffraction (XRD) spectra was obtained by using a Bruker D8 ADVANCE (Bruker, Germany) (CuK_α radiation with λ=1.5406 A°) with a 2θ scan range of 2° to 80° at room temperature. Morphology of samples was obtained by Scanning Electron Microscopy (SEM) (LEO 1430VP, Germany) and energy dispersive X-ray photoelectron spectroscopy (EDXS) respectively. Electrochemical properties of hybrid nanocomposites was studied using CH instrument model CHI1102A, in which glassy carbon (3 mm diameter), platinum and Saturated Calomel Electrode (SCE) was used as working, counter and reference electrodes respectively.

Synthesis of polyaniline (PANI) by chemical oxidation method

Aniline (2.0 g, 2.1mmol) and maleic anhydride (1g, 1.02mmol) were added into 150 mL water with stirring in an ice-water bath. After the mixture had been stirred for further 30 min to ensure to be cooled to 0°C, 50 mL aqueous solution of Ammonium peroxydisulfate (containing 6.54 g or 2.86mmol of Ammonium peroxydisulfate) was added into the mixture drop-by-drop. The polymerization was allowed to proceed for 24 h. The products were separated by centrifugation, then washed with water and ethanol, and dried at room temperature [yield: 62%]. (For PANI: FT-IR (KBr) υ: 3400, 1700, 1546, 1490, 1309 and 1147 cm^{-1})

Synthesis of polyaniline - polystyrene composite by in situ polymerization

To avoid the de doping of maleic acid (MA) molecules from the maleic acid doped PANI (PANI–MA), the radical bulk polymerization was conducted with a temperature gradient. The reaction mixture containing 0.50 g PANI–MA and 30.0 mL Styrene (27.27g, 26.2mmol) was heated at 40 °C, 50 °C, 60 °C and 70 °C for 2 days under stirring respectively, with 0.10 g BPO added upon each time to increase temperature except that 0.20 g BPO was added for 40 °C. Then the mixture was sealed and heated at 80 °C for 5 days and 100 °C for 2 days. The black PANI-polystyrene (PANI-PS) composite was obtained [yield: 40%]. (FTIR (KBr) υ: 1492, 1589, and 1633 cm^{-1}).

Synthesis of hybrid nanocomposite of polyaniline – polystyrene – chitosan/zinc oxide (PANI-PS-Chitosan/ZnO)

0.25 g of chitosan dissolved in 50 mL of acetic acid 4% and was stirred vigorously for 1 h. Then 50 mL (2.5% w/v)

solution of $ZnCl_2$ was prepared, added to chitosan solution and stirred continuously for 1 h at 80 °C. A light yellow viscous solution was formed. With this solution, 2 M NaOH (50 mL) was added into white precipitate and allowed to settle for 24 h. The supernatant solution was discarded and the precipitate (chitosan / ZnO nanocomposite) was rinsed with double distilled water for several times. Then dissolved in distilled water again and was labeled beaker (A). separately, into a beaker (it was labeled beaker B), 0.5 g of PANI-PS composite was added and Finally, the solution (A) slowly poured into a beaker (B) with stirred 20 min, and settled for 24 h to complete chemical reaction followed by washed more times with distilled water, filtered and dried at 80 °C (FTIR (KBr) υ: 2243, 1645 cm^{-1}).

RESULTS AND DISCUSSION

In the chemical oxidative polymerization of aniline in the present work, maleic anhydride reacted with water to produce maleic acid (MA) as both the dopant. PANI is known to consist of an imine and amine unit. Oxidative polymerization of aniline yields PANI of the Emeraldine structure having both amine and imine units (Scheme 1). However, other structures such as Leucoemeraldine and Pernigraniline are also possible.

In situ radical bulk polymerization was conducted with a temperature gradient to avoid the de doping of MA molecules from PANI–MA. The PANI had excellent aqueous-dispersibility but they cannot be dispersed into styrene. It is interesting to find that the mixture of the in situ radical bulk polymerization of styrene (St) in the presence of the PANI–MA became a stable dispersion after the polymerization stage at 60 °C. Furthermore, the viscosity of the polymerizing dispersion increased and the dispersion stability enhanced therefore after the polymerization stage at 70 °C. Subsequently, the radical bulk polymerization was completed by being heated at 80 °C and 100 °C, subsequently. The dispersibility of the PANI–MA in the PANI/PS composite was also analyzed with SEM. The PANI–MA was found to be dispersed uniformly in the PS matrix as the small aggregates with size less than 5 μm (Fig.1).

The TGA was conducted to measure the grafting of PS from the PANI–MA via copolymerization with the MA molecules (Fig. 2). The PANI–MA, and PANI–PS showed the weight losses of about 8.5% and 5.8%

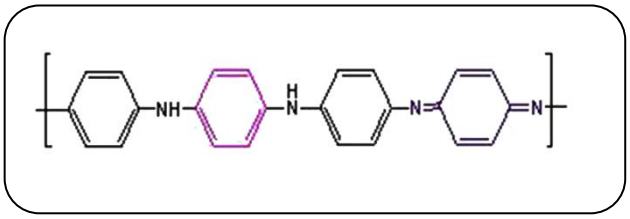

Scheme 1: Emeraldine structure.

respectively, due to the release of solvent and/or de doping of the dopant. The PANI–PS had a distinct weight loss at the temperature range from 150 °C to 300 °C, compared with the PANI-MA. It was attributed to the thermal decomposition of the grafted copolymer of St and MA with lower relative molecular weight.

UV-vis absorption spectra of PANI-PS-chitosan / ZnO hybrid nanocomposite is shown in Fig. 3. For PANI-chitosan composite three absorption bands at 292, 361, 575 nm have been observed. The lower wavelength band is associated with the π→π* transition of the conjugated ring systems and the longer wavelength band is assigned to the benzenoid to quinoid excitonic transition. In comparison to PANI-PS-chitosan /ZnO hybrid nanocomposite, the absorption bands at 292, 361 nm have blue-shifted and the absorption bands at 575 nm, red-shifted for hybrid nanocomposite, indicating the shifting of the absorption bands and thus strong interactions between chitosan-PANI and ZnO. Such kind of shifting of the absorption peaks due to the interaction between PANI and ZnO was also previously reported by Ref [37].

The crystallinity of PANI-PS-chitosan / ZnO hybrid nanocomposite and PANI-chitosan were analyzed using XRD measurements. The X-ray diffractograms of the PANI-chitosan polymer show distinct crystalline peaks attributed to chitosan and PANI, indicated by the presence of a broad peak at around 11.2° (Fig. 4) in agreement with the characteristic diffractogram of the original chitosan. The peak, appearing at around (20–30°), was assigned to the overlapping of chitosan with PANI and the peaks became broad is due to the presence of the PANI-chitosan composite. PANI-PS-chitosan / ZnO hybrid nanocomposite in the curve (b) shows all peaks belonging to the hexagonal wurtzite structure of ZnO nanoparticles with JCPDS (No. 36-1451) along with a small defined broad peak at 2θ = 15–27° belonging to PANI-chitosan. The peaks present in ZnO were also observed in all the compositions of PANI-PS-chitosan /

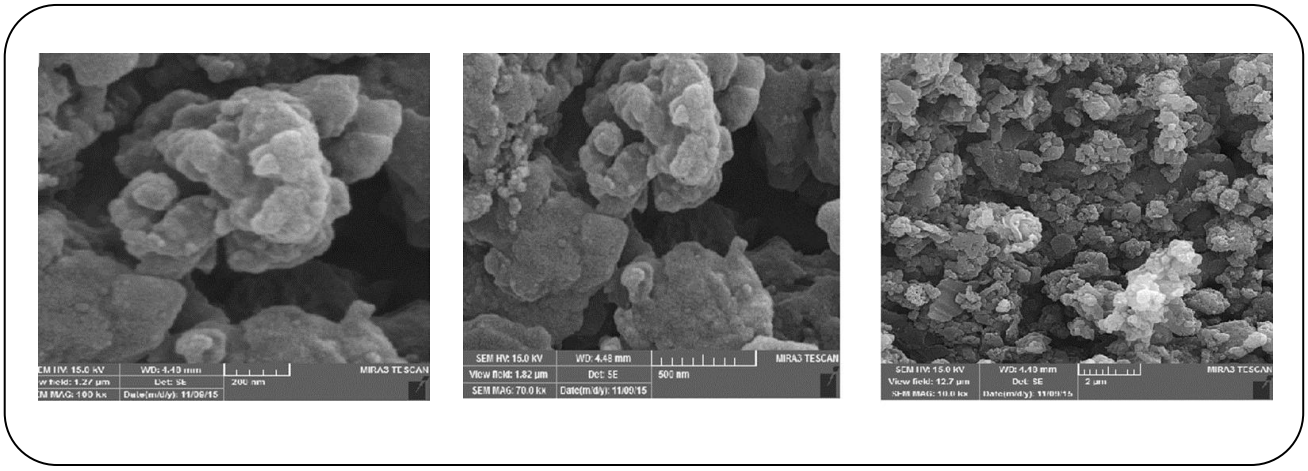

Fig. 1: SEM image of the PANI-PS composite.

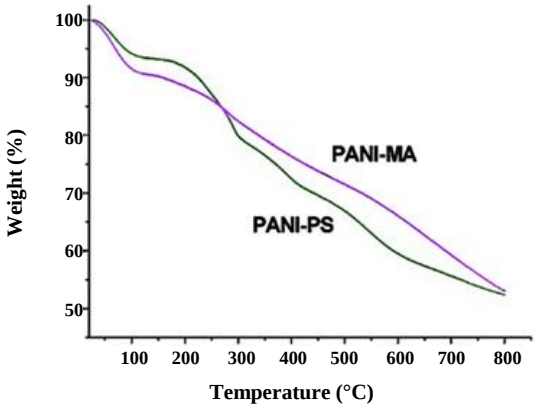

Fig. 2: TGA curves of the PANI–MA, and PANI– PS nanorods.

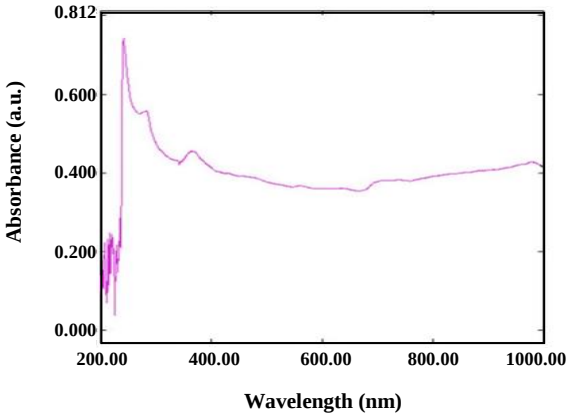

Fig. 3: UV-vis absorption spectra of PANI-PS-chitosan / ZnO hybrid nanocomposite in chloroform ($CHCl_3$).

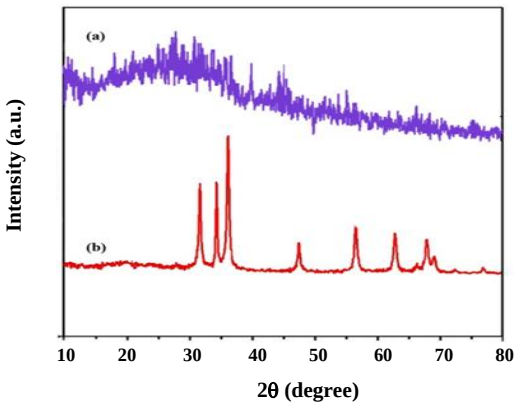

Fig. 4: XRD patterns of hybrids: (a) PANI-chitosan and (b) PANI – PS – chitosan / ZnO hybrid nanocomposite.

ZnO hybrid nanocomposite, which indicates the presence of nanoparticles in the polymer matrix. This result indicates that the crystal structure of ZnO has not changed after the mixing of PANI-PS on the chitosan/ZnO nanocomposite. The average crystallite size of the hybrid nanocomposite particles found using the values of FWHM was 79.4 respectively.

The morphological features of PANI-PS-chitosan / ZnO hybrid nanocomposite were analyzed through SEM analysis are shown in Fig. 5. The SEM images of the incorporation of ZnO nanoparticles into the PANI-chitosan matrix has uniform granular porous morphology attributed to the homogenous dispersion of ZnO nanoparticles in PANI-PS-chitosan / ZnO matrix as shown in Fig. 5. This indicates the PANI-PS-chitosan

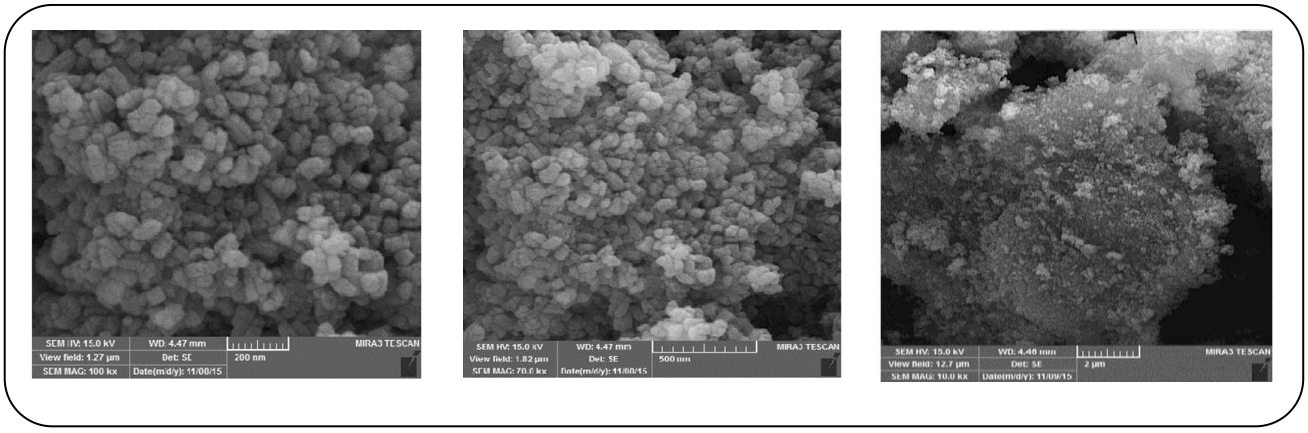

Fig. 5: SEM images of the PANI-PS-chitosan / ZnO hybrid nanocomposite.

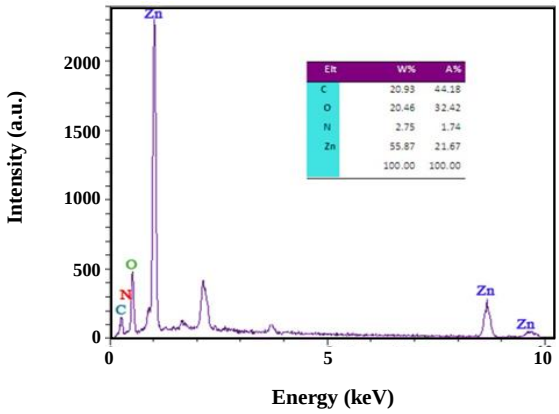

Fig. 6: Elemental analysis for PANI-PS-chitosan / ZnO hybrid nanocomposite by EDAX.

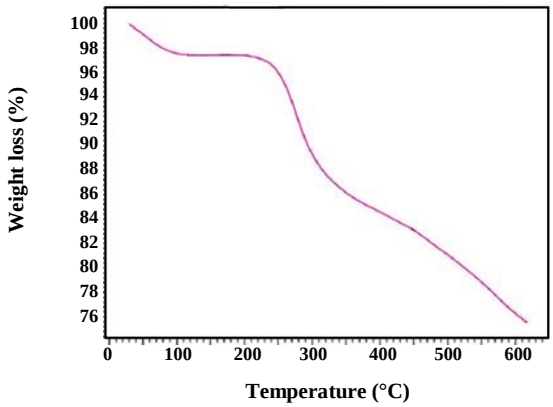

Fig. 7: TGA thermogram of PANI-PS-chitosan / ZnO hybrid nanocomposite.

polymer chains enclose the ZnO nanoparticles and the nanocomposites grow as multiparticle. The same observations can be found in the literature [38].

Presence of elements in the hybrid composite was analyzed by EDXS spectrum that was presented in Fig. 6. It exhibits peaks at 0.24, 0.36 and 0.52 keV corresponding to carbon, nitrogen, and oxygen respectively. The peaks are seen at 1.0, 8.6 and 9.6 are due to the presence of Zn. The weight ratios obtained from EDXS of PANI-PS-chitosan / ZnO hybrid nanocomposite are C, 20.93%; N, 2.75%; O, 20.45%; Zn, 55.87% respectively.

Thus clearly shows the presence of C, N, O, and Zn which indicates that both polymer and ZnO are present in the hybrid nanocomposites.

ThermoGravimetric Analysis (TGA) of PANI-PS-chitosan / ZnO hybrid composite is given in Fig. 7. The TG curve of the hybrid composite showed three stages of weight loss. The first stage occurred at 25-120°C with a weight loss of 2.67%, which was consistent with the loss of residual water from the material. The second stage involved a sharp and considerable weight loss at 120-450°C with a total weight loss of 14.27%, is attributed to the loss of PS chain grafted from the surface of PANI-PS composite. Final weight loss starts above 450°C, is ascribed to the degradation of the polymer chain.

Cyclic Voltammetry (CV) is a prominent tool to study the electrochemical properties of the material. The influence of ZnO within the redox behavior of PANI is investigated with the help of CV curves in the potential window of -0.2 to 0.8 V using 1 M of H_2SO_4 as the electrolyte. The CV curve of PANI-PS-chitosan / ZnO hybrid nanocomposite electrodes is presented in Fig. 8 at a scan rate of 100 mV/s. The CV curve of PANI-PS-chitosan / ZnO hybrid nanocomposite has three pairs of redox peaks; the first couple of peaks corresponds to the inter-conversion from Leucoemeraldine to Emeraldine ;

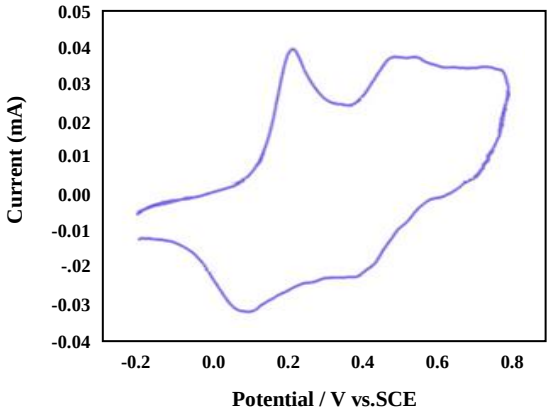

Fig. 8: Cyclic voltammograms of synthesized hybrid nanocomposite at a scan rate of 100 mV/s in 1 M H_2SO_4.

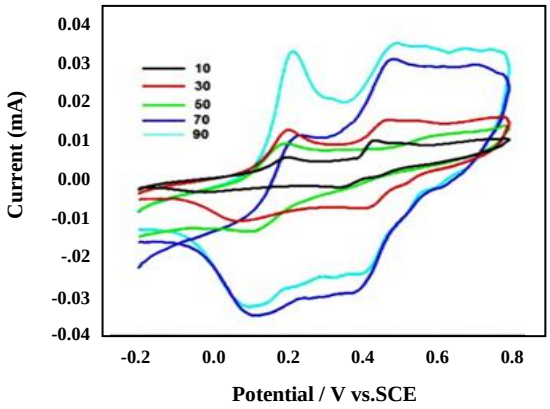

Fig. 9: Cyclic voltammograms of at various scan rates (10, 30, 50, 70 and 90 mV/s) in 1 M H_2SO_4.

a second couple of peaks is associated with the formation of benzoquinone and hydroquinone as additional products from aniline polymerization ; a third couple of peaks can be related to oxidation from Emeraldine to Pernigraniline . During the redox process, the current value for the PANI-PS-chitosan / ZnO hybrid nanocomposite was significantly increased. The lower current values of the redox peaks may be originated from the large portion of PANI molecules that are easily oxidized by being adsorbed on ZnO nanoparticles. The similar lower current values of the redox peaks of PANI were observed for higher amounts of palladium, carbon and TiO_2 nanoparticles. Fig. 9 shows CV obtained for PANI – PS – chitosan / ZnO hybrid nanocomposite at various scan rates of 10, 30, 50, 70 and 90 m/Vs. Further, with an increase of scan rate, a positive shift of oxidation, peaks are observed, which is mainly due to the resistance of the electrode.

CONCLUSIONS

The hybrid nanocomposite composed of PANI – PS – chitosan / ZnO was synthesized *via* simple in situ polymerization. This hybrid nanocomposite was analyzed for its structure, surface morphology, thermal stability and electrical property using various analytical techniques. The interaction between polyaniline-polystyrene and polyaniline-polystyrene-chitosan and ZnO and the nature of growth were investigated with the results of FT-IR.

The prominent shift in UV-Vis spectra indicates the formation of PANI – PS – chitosan / ZnO hybrid nanocomposites. From SEM analysis, it was observed that hybrid nanocomposite has a different morphological structure. The PANI–MA was found to be dispersed uniformly in the PS matrix as the small aggregates with a size of less than 5 µm. The SEM images of PANI-chitosan indicate that the particles are in lump fiber-like structure, whereas the incorporation of ZnO nanoparticles into the PANI-chitosan matrix has uniform granular porous morphology attributed to the homogenous dispersion of ZnO nanoparticles in the PANI-PS-chitosan / ZnO matrix.

XRD results show that the PANI – PS – chitosan / ZnO hybrid nanocomposite has better crystallinity than that of PANI-chitosan composite. The average crystallite size of the hybrid nanocomposite particles found using the values of FWHM was 79.4 respectively. EDAX clearly shows the presence of C, N, O, and Zn which indicates that both polymer and ZnO are present in the hybrid nanocomposite. The improved thermal and electrochemical performance in the present study maybe used in the future for various applications.

Acknowledgments

The authors thank Tabriz Payame Noor University for support of this project.

Abbreviations

BPO	Benzoyl peroxide
EDXS	Energy-dispersive X-ray photoelectron spectroscopy
FT-IR	Fourier- Transform Infra-Red
MA	Montmorillonite

PANI	Polyacrylonitrile
PS	Polystyrene
SEM	Scanning Electron Microscopy
St	Styrene
TGA	Thermogravimetric Analysis
UV-vis	Ultra Violet-Visible
XRD	X-Ray Diffraction

Received : May 21, 2018 ; Accepted : Aug. 27, 2018

REFERENCES

[1] Shabanian M., Khoobi M., Hemati F., Khonakdar H.A., Ebrahimi E, Wagenknecht U, Shafiee A., New PLA/PEI-Functionalized Fe_3O_4 Nanocomposite: Preparation and Characterization, *Journal of Industrial and Engineering Chemistry*, **24**: 211-218 (2015).

[2] Shabanian M., Khoobi M., Hemati F., Khonakdar H. A., Faghihi K.H., Wagenknecht U., Sadat Ebrahimi E., Shafiee A., Effects of Polyethyleneimine-Functionalized MCM-41 on Flame Retardancy and Thermal Stability of Polyvinyl Alcohol, *Particuology*, **19**:14-21 (2015).

[3] Khoobi M., Khalilvand-Sedagheh M., Ramazani A., Asadgol Z., Forootanfar Hand., Faramarzi M. A., Synthesis of Polyethyleneimine (PEI) and β-Cyclodextrin Grafted PEI Nanocomposites with Magnetic Cores for Lipase Immobilization and Esterification, *Journal of Magnetism and Magnetic Materials*, 375–384 (2014).

[4] Motevalizadeh F., Khoobi M., Sadighi A., Khalilvand-Sedagheh M., Pazhouhandeh M., Ramazani A., Faramarzi M. A, Shafiee A., Lipase Immobilization onto Polyethylenimine Coated Magnetic Nanoparticles Assisted by Divalent Metal Chelated Ions, *Journal of Molecular Catalysis B: Enzymatic*, **120**: 75-83 (2015).

[5] Akrami M., Khoobi M., Khalilvand-Sedagheh M., Haririan I., Bahador A., Faramarzi M. A., Rezaei S.H., Akbari Javar H., Salehi F., Kabudanian Ardestani S., Shafiee A., Evaluation of Multilayer Coated Magnetic Nanoparticles as Biocompatible Curcumin Delivery Platforms for Breast Cancer Treatment, *RSC Adv*., **5**: 88096-88107 (2015).

[6] Nobrega M. M., Izumi C. M.S., Temperini M. L.A., Probing Molecular Ordering in the HCl-Doped Polyaniline with Blk and Nano Fiber Morphology by Their Thermal Behavior, *Polym. Degrad. Stabil*., **113**: 66-71(2015).

[7] Hosseini M., Bahmani B., Moztarzadeh F., Rabiee M., Fabrication of a Sulfite Biosensor by the Use of Conducting Polymer, *Iranian Journal of Chemistry and Chemical Engineering (IJCCE)*, **27** (1): 115-121. (2008).

[8] Babar D. G., Olejnik R., Slobodian P., Matyas J., High Sensitivity Sensor Development for Hexamethylphosphoramide by Polyaniline Coated Polyurethane Membrane Using Resistivity Assessment Technique, *Measurement.*, **89**: 72-77 (2016).

[9] Pandiselvi K., Thambidurai S., Synthesis, Characterization, and Antimicrobial Activity of Chitosan–Zinc Oxide/Polyaniline Composites, *Materials Science in Semiconductor Processing*, 573-581 (2015).

[10] Zhao Y., Zhang Z., Yu L., Tang Q., Electrospinning of Polyaniline Microfibers for Anticorrosion Coatings: An Avenue of Enhancing Anticorrosion Behaviors, *Synthetic. Met*., **212**: 84-90 (2016).

[11] Kannusamy P., Sivalingam TH., ChitosaneZnO/Polyaniline Hybrid Composites: Polymerization of Aniline with Chitosane ZnO for Better Thermal and Electrical Property, *Polymer Degradation and Stability*, **98**: 988-996 (2013).

[12] Qiu H., Han X., Qiu F., Yang J., Facile Route to Covalently - Jointed Graphene/Polyaniline Composite and it's Enhanced Electrochemical Performances for Supercapacitors, *Appl. Surf. Sci*., **376**: 261-268 (2016).

[13] Saini P., Choudhary V., Singh B. P., Mathur R. B., Dhawan S.K., Enhanced Microwave Absorption Behavior of Polyaniline-CNT/Polystyrene Blend in 12.4–18.0 GHz range, *Synthetic. Met*., **161**: 1522–1526 (2011).

[14] Trépanier M., Tavasoli A., Sanaz Anahid S., Dalai A. K., Deactivation Behavior of Carbon Nanotubes Supported Cobalt Catalysts in Fischer-Tropsch Synthesis, *Iranian Journal of Chemistry and Chemical Engineering (IJCCE)*, 30(1): 37-47 (2011).

[15] Do J.S., Lin K.H., Ohara R., Preparation of Urease/Nano-Structured Polyaniline–Nafion (R)/Au/Al_2O_3 Electrode for Inhibitive Detection of Mercury Ion, *J. Taiwan. Inst. Chem. Eng*., **43**: 662–668 (2012).

[16] Kamalesh S., Tan P., Wang J., Lee T., Kang E. T., Wang C.H., Biocompatibility of Electroactive Polymers in Tissues, *J. Biomed. Mater. Res. Part A*, **52**: 467–478 (2000).

[17] Shi N., Guo X., Jing H., Gong J., Sun C., Yang K., Antibacterial Effect of the Conducting Polyaniline, *J.Mater.Sci.Technol*. **22**: 289–290 (2006).

[18] Pedro R. D. O., Takakia M., Gorayeb T. C. C., Bianchi V. L. D., Thomeo J. C., Tieraa M. J., De V. A., Tiera O., Application of Quaternary Derivatives of Chitosan as Bio Fungicide About Fungus 'Aspergillus flavus', *Microbiol. Res*. **168**: 50–55 (2013).

[19] Chen C. H., Dai Y. F., Effect of Chitosan on Interfacial Polymerization of Aniline, *Carbohydr. Polym*. **84**: 840–843 (2011).

[20] Jeon Y. J., Park P. J., Kim S. K., Antimicrobial Effect of Chitooligosaccharides Produced by Bioreactor, *Carbohydr. Polym*. **44:** 71–76 (2001).

[21] Sawai J., Yoshikawa T., Quantitative Evaluation of Antifungal Activity of Metallic Oxide Powders (MgO, CaO and ZnO) by an Indirect Conductimetric Assay, *J. Appl. Microbiol*. **96**: 803–809 (2004).

[22] Krishnaveni R., Thambidurai S., Industrial Method of Cotton Fabric Finishing with Chitosan–ZnO Composite for Anti-Bacterial and Thermal Stability, *Ind. CropsProd*. **47**: 160–167 (2013).

[23] Palaniappan S., John A., Novel Polyaniline – Fluoroboric Acid –Dodecylhydrogensulfate salt: Versatile Reusable Polymer Based Solid Acid Catalyst for Organic Transformations, *J. Mol. Catal. A-Chem*,, **233**: 9-15 (2005).

[24] Ryu K.S., Moon B.W., Joo J., Chang S.H., Characterization of Highly Conducting Lithium salt Doped Polyaniline Films Prepared from Polymer Solution, *Polymer*., **42**: 9355-9360 (2001).

[25] Izumi C. M. S., Constantino V. R. L., Ferreira A.M. C., Temperini M. L. A., Spectroscopic Characterization of Polyaniline Doped with Transition Metal Salts, *Synthetic Met.*, **156***:* 654-663 (2006).

[26] Dimitriev O.P., Interaction of Polyaniline and Transition Metal Salts: Formation of Macromolecular Complexes, *Polym. Bull*., **50**: 83-90 (2003).

[27] Abbasian M., Jaymand M., Niroomand P., Farnoudian-Habibi A., Ghasemi Karaj-Abad S., Grafting of Aniline Derivatives onto Chitosan and Their Applications for Removal of Reactive Dyes from Industrial Effluents, *International Journal of Biological macromolecules*, **95**: 393-403(2017).

[28] Abbasian M., Mahmoodzadeh F., Synthesis of Antibacterial Silver–Chitosan-Modified Bionanocomposites by RAFT Polymerization and Chemical Reduction Methods, *Journal of Elastomers & Plastics*, **49** (2): 173-193 (2017).

[29] Abbasian M., Niroomand P., Jaymand M., Cellulose/Polyaniline Derivatives Nanocomposites: Synthesis and Their Performance in Removal of Anionic Dyes from Simulated Industrial Effluents, *Journal of Applied Polymer Science*, **134**: 45352 (2017).

[30] Abbasian M., Pakzad M., Nazari K., Synthesis of Cellulose-Graft-Polychloromethylstyrene-Graft-Polyacrylonitrile Terpolymer/Organoclay Bionanocomposite by Metal Catalyzed Living Radical Polymerization and Solvent Blending Method, *Polymer-Plastics Technology and Engineering.*, **56** (8): 857-865 (2017).

[31] Abbasian M., Pakzad M., Ramazani A., Nazari K., Cellulose Modification Through Grafting of Polyacrylonitrile by Atom Transfer Radical Polymerization, *Iranian Journal of Polymer Science and Technology*, **28** (4): 323-332 (2015). [in Persian]

[32] Abbasian M., Mahmoodzadeh F., Synthesis of Chitosan-Graft-Poly (Acrylic Acid) Using 4-Cyano-4-[(Phenylcarbothioyl) Sulfanyl] Pentanoic Acid to Serve as RAFT Agent, *Journal of Polymer Materials*, **32** (4): 527 (2015).

[33] Karaj-Abad S.G., Abbasian M., Jaymand M., Grafting of Poly [(methyl methacrylate)-block-styrene] onto Cellulose *via* Nitroxide-Mediated Polymerization, and its Polymer/clay Nanocomposite, *Carbohydrate Polymers*, **152**: 297-305 (2016).

[34] Xuan H., Yao C., Hao X., Liu C. et al., Fluorescence Enhancement with One-Dimensional Photonic Crystals/Nanoscaled ZnO Composite Thin Films, *Colloid. Surface. A.*, **497**: 251-256 (2016).

[35] Yadollahi M., Farhoudian S., Barkhordari S, Gholamali I., Farhadnejad H., Motasadizadeh H., Facile Synthesis of Chitosan/ZnO Bio-Nanocomposite Hydrogel Beads as Drug Delivery Systems, *Int. J. Biol. Macromol*., 82: 273-278 (2016).

[36] Ghasemi M., Elaheh Kowsari E., Ali Amoozadeh, Chitosan/Poly(Amide-Imide) Blend Films: Studies on Thermal and Mechanical Stability, Morphology and Biodegradability, *Iranian Journal of Chemistry and Chemical Engineering (IJCCE)*, **36**(2), 55-70 (2017).

[37] Xu J. C., Liu W. M., Li H.L., Titanium Dioxide Doped Polyaniline, *Mater. Sci. Eng. C.*, **25**: 444-447 (2005).

[38] Salem M. A., Al-Ghonemiy A. F., Zaki A. B., Photocatalytic Degradation of Allura Red and Quinoline Yellow with Polyaniline/TiO_2 Nanocomposite, *Appl. Catal. B.*, **91:** 59-66 (2009).